Impact Assessment of common-Mode interference on communication cable in a Motor Drive System: Modified Bulk Current Injection Approach

Kushan Choksi, Yuxuan Wu, Deepi Singh, and Fang Luo
Department of Electrical and Computer Engineering
Stony Brook University
Stony Brook, NY, USA

choksi.kushan@stonybrook.edu, yuxuan.wu@stonybrook.edu, deepi.singh@stonybrook.edu, fang.luo@stonybrook.edu

Abstract—Adjacent communication network coupling disturbances due to conducted electromagnetic interference (EMI) coupling and near field coupling is a growing concern for highfrequency motor drives. The performance of the communication network is majorly compromised due to considerable commonmode (CM) current induced into communication cable due to high dV/dt and di/dt of wide band gap (WBG) devices-based motor drives. Estimation of such CM current is a non-trivial task owing to the complex coupling mechanism between the motor drive cables and the communication network. This paper studies the EMI noise problem in a WBG device's motor drive varying with grounding mechanism and layout design. Firstly, the impact of grounding has been explored on conducted and near-field (NF) radiated noise propagation paths. This paper uses high precision dobot (robotic arm) based near field sniffing mechanism for the same Secondly, a high-frequency cable and motor modeling technique is introduced to predict the EMI noise source and propagation path. This paper uses impedance analysis and Ansys Q3D Extractor is a parasitic extraction tool-based approach for modeling. Lastly, the paper also provides a novel modified bulk current injection testing (MBCI), and NF mapping technique has been provided to explore the adverse impact of EMI coupling on communication cables. This is an empirical, simpler, and cost-efficient approach for analysis, estimation, and mitigation of the common mode coupling between motor drives and adjacent communication networks.

Index Terms—Common-mode (CM) current coupling, communication network, coupling mechanism, electromagnetic interference (EMI) modeling, modified bulk current injection

I. INTRODUCTION

Rapid electrification of the transportation and aircraft industry in recent years has led to demand for high power density and efficiency in power electronics motor drives. Advancements in wide band-gap device technologies have sufficed these demands at the cost of high-frequency (EMI) noise and high-power density packaging [1]. This interaction of electromagnetic (EM) fields has raised concerns about electromagnetic compatibility, communication, and control signals. Despite a good understanding of conducted EM emissions due to high voltage and current slew rate (dV/dt and di/dt), there are concerns about the impact of shields and various communication interfaces in the practical world [2]. However, near-field radiated emissions are not well understood as they can

case specific and set up specific [2]. Communication errors can be fatal in high frequency, high-power density, and compact environments. Logical errors, communication delays, and signal jitters resulting by electromagnetic couplings between the motor drive and the communication circuit induce CM current in communication cables. They can lead to failed controls, sensing, and health monitoring signal networks. Commonly used solutions are using shields, EMI chokes, and Y caps.

However, this solution has four major issues: 1) Most analyses and optimization for motor drives do not consider the rest of the system, such as the dc power supply circuit and the communication circuit optimization leading to high volumes of CM chokes [2]; 2) the design methods of these solutions are mostly empirical but without consideration of variance in infrastructure and accurate near field modeling [3]; 3) the optimizing procedure of the CM chokes and shielded cables are time-consuming and complex without significant studies of EMI coupling 4) Some solutions are prone to inductive coupling, enclosure slots serving as antennas, and quality of grounding [3]. Hence, it is important to find simpler, automated, and less time-consuming empirical understanding tools to draw a measurable and extendable relationship between practical aspects and theory. Moreover, there is a need for accurate modeling as well as a simpler method to deal with both conducted and radiated emissions and their associated coupling phenomenon with varying infrastructure and grounding mesh [4].

Plenty of detailed research has been done in the domains of EMI modeling and analysis. However, the impact of shielding/grounding with long cable motor drives remains a research gap. In terms of radiated emission scanning for motor drives focused on the EMI models of motor and communication circuits [1]- [5]. However, coupling mechanisms and communication architecture in terms of pitch angles, orientation, and type of cables have not been summarized in detail. Also, a simpler indicative method for the coupling mechanism remains to be a gray area. Lastly, DM to CM transformation exploration must be better understood, especially when colliding with high-frequency phenomena like the skin effect, proximity effect, and reflected waves in long cable motor

drives. In the RS485 communication line, high differential-mode (DM) voltage induces in RS cables due to high CM currents in GND cables because of asymmetries in the printed circuit board (PCB) parameters components of the RS485 communication circuit. This superimposition of DM voltage degrades communication performance.

The main aim of this work is to illustrate and investigate EM coupling between motor drives and adjacent communication networks. The major contribution of this work is as follows: 1) Investigation and evaluation of the impact of grounding on radiated and conducted emissions for the high-frequency motor drive system. 2) Accurate and precise heat map extraction for analysis of radiated EMI using a Dobot robotic arm. The idea is to analyze the impact of grounding, shield, cable lengths, and cabling infrastructure on CM coupling mechanisms. 3) Paper provides concrete modeling of cable motor and converter for accurate prediction of conducted as well as radiated EMI. Conducted emissions were predicted using impedance analysis, whereas radiated emissions were modeled using Ansys Q3d. 4) Lastly, a novel modified bulk current injection method provides for analysis of the impact of communication line placement and architecture for minimum coupling, aiding to least communication jitter due to CM noises. This is a simple, cabling infrastructure extendable and non-time-consuming evaluation technique for understanding the impact of cabling variation on communication cables in motor drives.

II. COMMUNICATION CABLE NOISE COUPLING: MODEL

A standard communication networked motor drive system can be envisioned as shown in Fig. 1. Communication cables

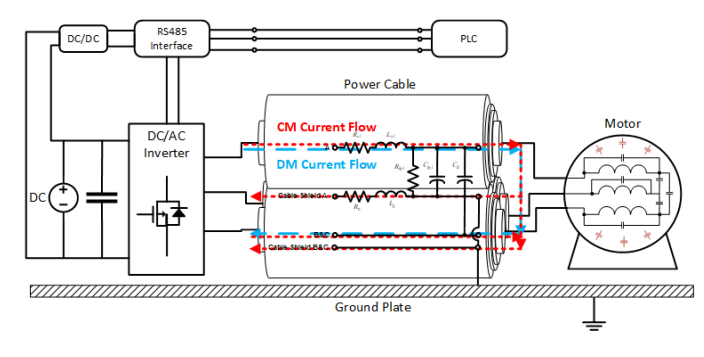


Fig. 1. Typical motor drive system with communication network

are susceptible to noise coupling from a motor drive in three major ways: 1) EMI CM current coupled to communication GND cable and dc-dc stage of motor drives. 2) CM EMI of the motor drive will couple to the communication cables through near-field coupling. 3) Far-field coupling in case of shield slot antenna formations. In order to investigate the communication coupling mechanism, we used a long cable motor drive system prototype with RS485 communication cables. These cables are supposed to connect between RS485 module and the programmable logic controller (PLC). This

paper uses a 50-ohm load to terminate the RS 485 cable to ensure we only investigate and evaluate how motor drive components/ parasitic influence the signal noise.

It shall be noted that Fig. 1, shows CM and DM conducted noise path for a long cable motor drives system. Also, normally, communication cables are placed very close to the motor drive system leading to minimal chances of far-field coupling. Hence this paper will explore CM conducted noise propagation path and near field coupling path.

A. Conducted Coupling Model

The CM EMI of the inverter couples with the communication cable using the common ground path, as shown in Fig. 1. The inverter noise couples through a path including dc/dc converter, RS485 module ground, communication cables, PLC, and the earth/round/PE. The dc-dc converter is the dominant EMI source, which according to Thevenin Theory is modeled by a voltage source and an internal impedance. Two voltage sources to represent conducted EMI coupling are U_{DM} and U_{CM} for the dc-dc and bus mid-point CM noise source. U_{CM} is the noise voltage between the drain-source of MOSFET as shown in Fig. 2.

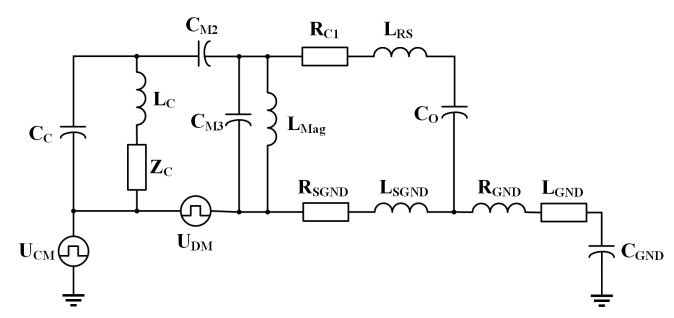


Fig. 2. Approximate CM conducted EMI Estimation Modeling

 L_{mag} is the magnetizing inductance for the dc-dc stage isolation. Since the dv/dt is very low for communication, unlike the power circuit, the interference source RS486 and PLC converter can be ignored or considered negligible. The ground path plays an important role, which couples between the communication cable and the dc-dc stage of a motor drive. Also, the L_{mag} could be replaced by coupled inductor or isolation transformer model. This model can be used for the estimation of conducted inferences for the communication cable. However, it needs to be coupled with NF couple modeling for the estimation of accurate high-frequency noise.

B. Near-Field Coupling Mechanism

The proximity of communication cables leads to near-field coupling between the motor cable and the communication cable. Generally, communication cables are almost of the same length as the motor drive cable to ensure communication of data on the motor side and converter side sensors' feedback to the controller. The near-field coupling can be in the form of Efield and H-field, which can be seen as magnetic or capacitive coupling. The communication cables are kept close to the

motor cable leading to mutual coupling (H-field) between the motor cable and RS 485+- cables, ground cables, and motor ground cable and motor ground to RS 485+- cable represented as M_{LL} , M_{GG} , and M_{LG} respectively. The CM E-field coupling can be represented as C_1 , C_2 , C_3 , and C_4 , which may be power cable to communication cable, power earth to analog ground, power cable to analog ground and communication cable to power earth respectively as shown in Fig. 3. It shall be noted that Z_m , Z_s are motor and source

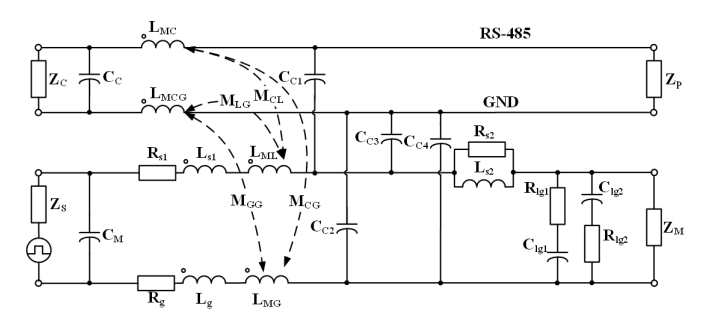


Fig. 3. Approximate Near Field Estimation Modeling

impedance. Whereas the parallel branch of L_{s2} , R_{s2} provides a flexible architecture, which leads to increased resistance at high frequency. This branch helps the cable model mimic the increased resistance and decreased current density due to the skin effect at cable conductors. It shall be noted that the series branch of C_{lg2} , R_{lg2} in parallel to C_{lg1} R_{lg1} provides a flexible architecture for incorporating the proximity effect. This leads to increased resistance at high frequencies between the conductor and the shield. The extraction of both the CM conducted and near field path is explained in detail in [6]. There is a notable role of CM noise in communication disruption. Hence it is paramount to understand the impact of grounding on motor drive EMI as well as the communication interface due to grounding.

III. EVALUATION OF FACTORS IMPACTING EMI COUPLING

Empirical experiments taking into consideration DO-160G have been conducted to determine a model and experimentbased assessment of the role of ground and shield. Conducted EMI as well as radiated near field (NF) EMI in a cable-connected motor drive system with different grounding schemes is measured in this section. For the conductive EMI testing, the output of the DC power source is connected to a line impedance stabilization network (LISN) complied with CISPR 25 standard, as shown in Fig. 4. It shall be noted that a three-phase inductive load represented motor load. The idea is to study the EMI interaction between the power and communication cables. Hence, using a pure inductor will allow for avoiding high-frequency resonance from motor parasites. The NF EMI is measured using an H-field probe with a signal amplifier, and the conductive EMI is measured with LISN with CM and DM noise separator mini circuit. The testing setup uses a three-phase motor drive with a low DC link voltage and

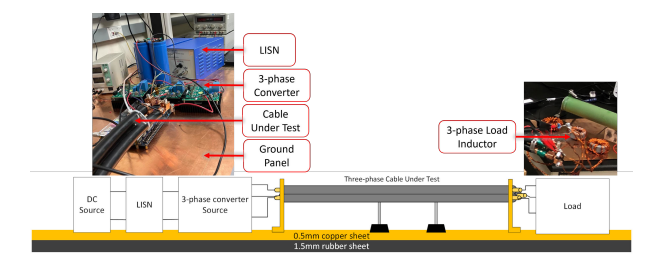


Fig. 4. Conductive EMI testing setup

large current setup for the comparative study. The cable under test is a set of 0 AWG shielded cables bundled into a three-phase in parallel with a 5 mm gap between each phase. By using the NF EMI testing setup presented in Fig. 5; the H-field probe is held by a robotic arm which is programmed to move in 1 cm step to capture the NF signal around the transmission line; the signal is captured with a spectrum analyzer and capturing the peak of NF EMI; a ground panel is used as reference ground for testing proposes. The list of components used is given in Table. I.

TABLE I EQUIPMENT USED FOR EXPERIMENTAL EVALUATION

Equipment/Component	Model
Cable under test	1/0 AWG Southwire 5 kV single
	conductor copper tape shielded cables
Impedance Analyzer	Omicron-lab Bode 100
Converter Switches	SiC MOSFET: NTHL080N120SC1
	GaN HEMT: GS66506T
Half-bridge Converter	Evaluation Boards:-
	CREE SiC half-bridge
	Lab Made GaN Half-bridge
Load Inductor	470uH Lab Made Air Core Inductor
Scope	Tektronix 5 Series Oscilloscope
Voltage Probe	Tektronix THDP0200 1500V 200MHz
Current Probe	Tektronix TCP0030 30A
Robotic Arm	Dobot Magician
LISN	CISPR LISN 25 A

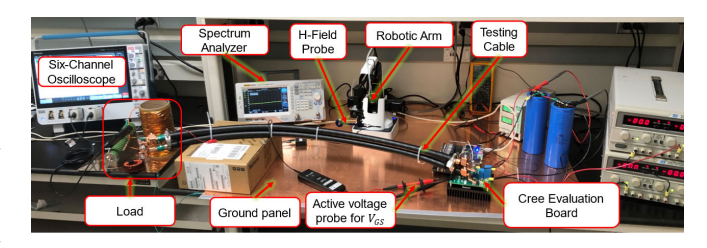


Fig. 5. Radiated EMI testing setup

A. The Impact of Grounding on EMI

This paper mainly studies various grounding schemes, including load-side grounding, source-side grounding, meshed grounding, and ungrounded cases. It was noticed that the grounding side plays a vital role in CM noise. It was noticed that ungrounded cable shows higher CM noise compared to other cases. However, the noise peak at high frequency

is high for Load-source grounding. It interferes with the communication channel frequency of 1.1 MHz in this case. This phenomenon can be because a long copper plane was used as ground, causing a loop when grounded on the side. The EMI propagated from this loop is causing concerns for communication channel coupling, as suggested in Fig. 6. Secondly, this paper studies the type of cable used in motor

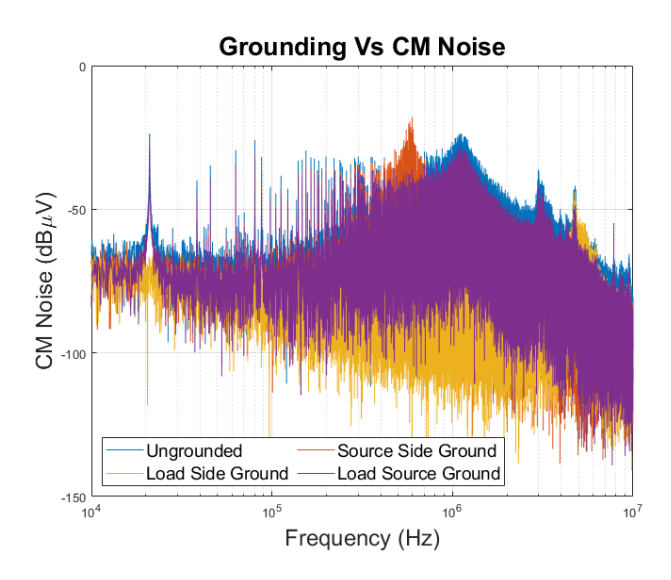


Fig. 6. CM Conducted Noise Vs Grounding Location

drives using FEA analysis using Q3d Ansys. four cases were studied: 1) Case 1: Three cables with individual shields; 2) Case 2: Common shield rubber-filled bundled cable; 3) Case 3: Common shield bundled cable without rubber filling, where insulation shield is removed and filled with air; and 4) Case 4: Bundled cable without a shield. Fig. 7: Common Mode

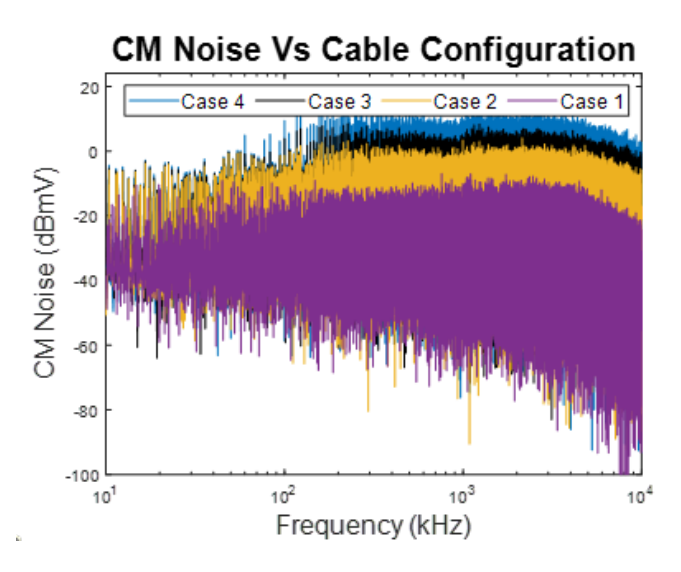


Fig. 7. CM Conducted Noise Vs Cable Configuration

Noise for Various Cable Configuration. The common mode noise is seen to be highest in case 4 and least in case 1 due to

lower line-ground capacitance. However, it was noted that no significant change was noticed in DM noise. It was noted that separately shielded cable generates 59% less common mode noise generation at higher frequency as opposed to unshielded cables. However, the difference is around 19% for frequencies less than 2 kHz. Hence it can be concluded that cables with three separate shielding layers are best for CM noise.

B. Impact of Near Field Emission

The near-field emissions were measured using both E-field and H-field probes. However, it was noticeable that the H-field emissions were much stronger. Hence, H-field and near-field emissions were used interchangeably for this investigation. The idea here was to create a mapping of H field generation throughout the length of the cable. This includes mainly 1) the Center of the cable, 2) the Load End of the cables, and 3) the Source end of the cable. This is just for achieving a generalization of magnetic coupling around symmetrically placed 3-ph motor cables. The result displayed in the paper is for grounded cable setup. Spiral tapped as well as braided shield cables with similar characteristics were used. It was

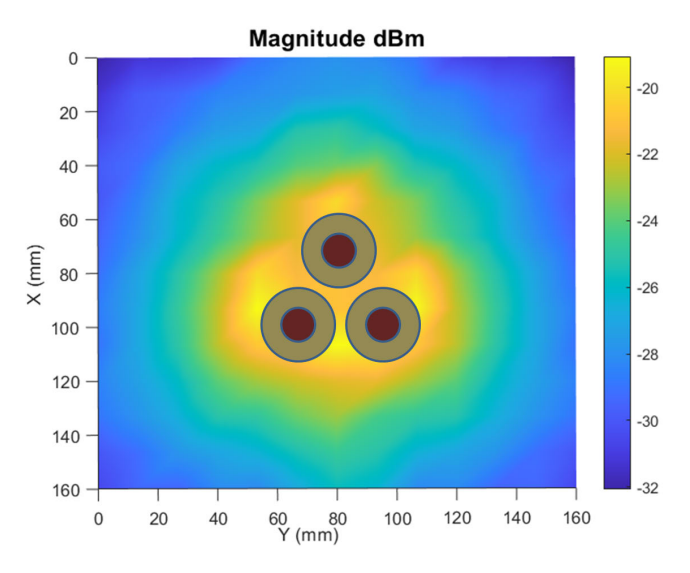


Fig. 8. Dobot based NF (dBm)Heat Map at Center of the cable

noted that the magnetic heat map trend did not change with the type of shield. The heat map was symmetrically distributed across the cables when projected from the center of the cable, as shown in Fig. 8. Fig. 8 shows that at the center of the cable the H-field was seen to be symmetric as well as significantly lower in magnitude. Whereas the NF was found to be stronger at the terminal, as shown in Fig. 9, also the trend suggested that the NF was heavily coupled toward the ground copper pane shared by both the communication cable as well as a motor power cable. The maximum radiation was found between cables, and a higher H-field was observed between cables and the ground panels, as presented in Fig 8,9. It was observed that the cable leads served as a monopole antenna which can be accounted responsible for higher NF at terminals. Also, NF

mostly couple towards the ground panel can be attributed to terminal end shielding. The first mitigation approach suggested is the introduction of a terminal box, which helped in the reduction of NF by 12 dBm. Secondly, place the communication cable away from the power terminal. However, this may not be a viable solution in practical scenarios where communication and power terminals share the same chassis.

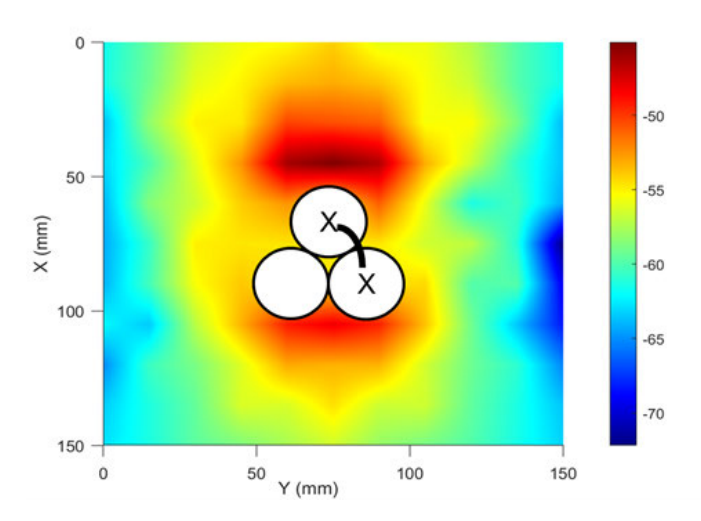


Fig. 9. Dobot based NF (dBm)Heat Map at terminal of the cable

This approach of estimation of the near field, despite being spatially accurate, also comes with its own challenges as follows: 1) Only one frequency can be observed at a time. It was 2 MHz for this work. 2) Maximum peak of radiation must be observed at every point to ensure comparability of various heat maps and locations; 3) Maxwell's equation can be used for the study of sensitivity and nature of radiation. This might be time-consuming and not very trivial. Hence there is a strong need for simpler and extendable estimation of communication interference which can be conducted radiated (H-field or E-field).

IV. MODIFIED BULK CURRENT INJECTION APPROACH

Modeling of noise path, high-frequency modeling of the system, and robotic arm based near field coupling approaches are time-consuming, complex, and yet infrastructure oriented. This approach can help build RF or CM filters which can get bulky. Lastly, these approaches are not always extendable to higher rating or cascading systems. In order to achieve an easy and extendable alternative for cross-talk estimation is proposed in this section. The idea is to devise an experimental empirical system that is repeatable, simple, and conclusive.

This approach is inspired by the Bulk current injection (BCI) approach, which is traditionally widely used for system immunity evaluation [7]. It is a conducted susceptibility (CS) test based on the injection of high-frequency common-mode (CM) noise currents in bundles of cables. It uses a BCI current transformer for the injection of high-frequency currents externally. It is considered a test method in the avionic

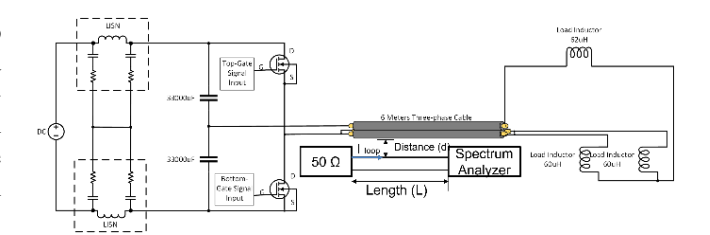


Fig. 10. Schematic setup for modified bulk current injection test

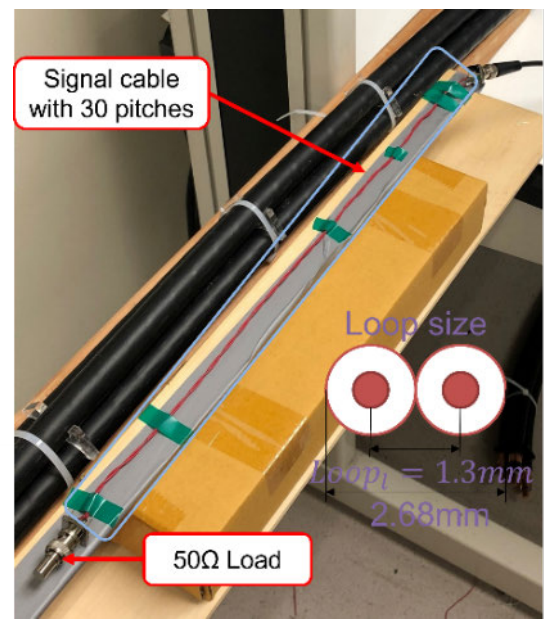


Fig. 11. MBCI test setup and Loop size definition

standard DO-160, automotive standard ISO 11452-4 [8], and the military standard MIL-STD461 [9]. It is considered an alternative method to direct injection in IEC 61000-4-6 [8].

A modified BCI (MBCI) testing is proposed in the paper for evaluating the coupling between communication lines and power cables. The idea is to capture high-frequency common mode current in the communication cable injected wire power cables. This is the opposite interpretation of the source and victim of the BCI test. This test deals with the power cable as the source of CM current and communication cables as the victim. The modified BCI testing uses a power cable as a noise source and places a signal cable next to it to replicate the interference from a power cable to a signal wire. The signal wire loop is terminated with a 50 Ω resistor and connected to an oscilloscope, as presented in Fig. 11. The CM currents and the victim loop currents are shown if Fig. 12. A transfer gain is defined as the ratio of CM currents to coupled communication inferences in currents or voltages based on the application. This paper uses transfer gain as a ration of CM current in power cables to current coupled in the victim loop. This ratio can be monitored separately or used to explore the sensitivity of communication interferences to the length of the loop, the number of twists, and the

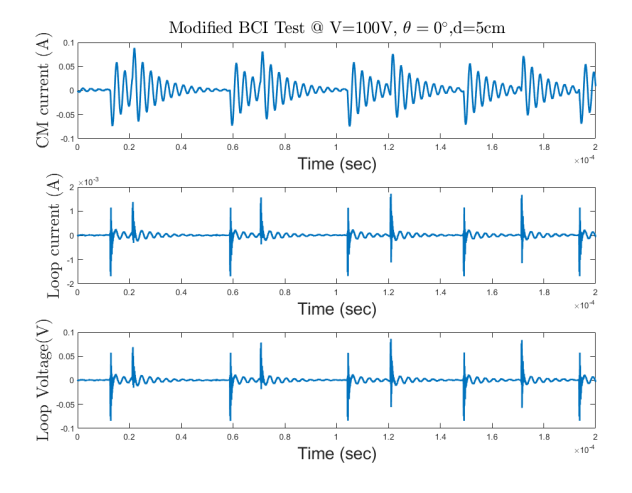


Fig. 12. CM currents Vs Victim loop currents for MBCI Test (theta=0 deg, distance=10 cm, loo length 2 meter)



Fig. 13. Transfer Gain Vs Communication cable Orientation

distance/location from the power cable. The MBCI test is highly susceptible to orientation, distance, and pitches (twists). This test can prove vital in two major dominions: 1) Finding location and orientation for minimum coupling of noise; 2) Studying the sensitivity of communication interference with various practical layout factors. MBCI testing can perform the measurement with various distances, signal loop sizes, positions, and signal wire pitches. Fig .13 shows the transfer gain when the signal cable, which has no pitch, lays out in a different orientation, and it shows that transfer gain is highly affected by the orientation angle. It can be established that the relationship would be a squared polynomial between transfer gain and theta angle varied from 0 to 90 degrees on either side of the horizontal plane. Fig .14 shows the transfer gains when the signal cable with different pitches while varying the distance between the power cables. It is evident that the coupling relation is decreasing exponentially

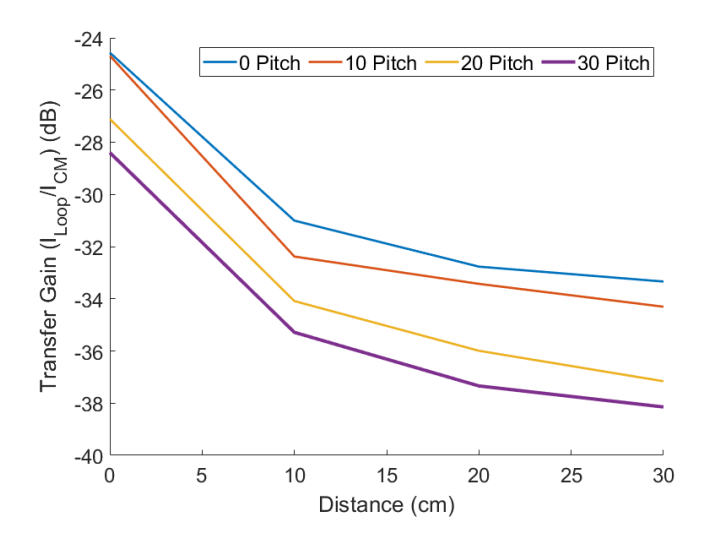


Fig. 14. Transfer Gain Vs No of Pitch

and saturates around 30 cm. It was observed that twisting communication cables with the increased number of twist pitch reduces transfer gain or communication interference.

Similarly, it was observed that transfer gains were having exponential, linear, and inverse exponential relationships with victim loop length, motor drive operating voltage, and distance from the power cable, respectively. If the CM mode currents increases at higher voltage levels distance of the power cable to the signal cable will be very relevant. The equations between transfer gain and various factors can be derived by exponential fit. Such equations can prove vital when it comes to the extension of methodology for different layouts and setups.

V. Conclusion

Communication cable disruption has been a long-standing issue in power-dense motor drive systems leading to control and monitoring failure. This paper deals with conducted and near-field radiated noise propagation, modeling, and estimation of high-frequency long cable motor drives. The impact of grounding architecture for shielded three cable motor drives is studied. It was noted that grounding both ends of a shielded cable may not be advisable, and grounding architecture must be decided as a function of the length of the cable, motor side chassis grounding, etc. The paper generates a heat map for analysis of near field EMI and coupling due to motor drive considering shielding framework. The heat map is generated using a robotic arm-based probing method with a resolution of 10 mm. It was noted that NF radiation was greater at the cable terminal, mostly toward the ground plane, owing to cable leads and grounding connections serving as monopole antennas.

A novel simplistic empirical approach is proposed for communication line near field coupling analysis. Transfer gain is used as a yardstick for the comparison of various cases. This is vital for finalizing the location, critical length, and orientation of the communication cable. It investigates the impact of communication loop size, shield, orientation, system power levels, victim loop diameter, etc. Lastly, this approach is significantly useful to identify if maintenance or layout change will impact the communication noise in the future without going through time-consuming modeling ad mitigation approaches.

REFERENCES

- [1] H. Chen, T. Wang, S. Ye, and T. Zhou, "Modeling and suppression of electromagnetic interference noise on motor resolver of electric vehicle," *IEEE Transactions on Electromagnetic Compatibility*, vol. 63, no. 3, pp. 720–729, 2020.
- [2] H. Chen and T. Wang, "Estimation of common-mode current coupled to the communication cable in a motor drive system," *IEEE Transactions* on *Electromagnetic Compatibility*, vol. 60, no. 6, pp. 1777–1785, 2018.
- [3] K. Choksi, Y. Wu, M. Ul Hassan, F. Luo, B. Liu, and X. Wu, "Inspecting impact of cabling infrastructure on reflected wave and emi for more electric aircraft (mea) motor drives," in 2022 IEEE Transportation Electrification Conference Expo (ITEC), pp. 529–533, 2022.
- [4] A. B. Mirza, A. I. Emon, S. S. Vala, and F. Luo, "Noise immune cascaded gate driver solution for driving high speed gan power devices," in 2021 IEEE Energy Conversion Congress and Exposition (ECCE), pp. 5366– 5371, 2021.
- [5] K. Choksi, Y. Wu, M. ul Hassan, and F. Luo, "Evaluation of factors impacting reflected wave phenomenon in wbg based motor drives," in 2022 International Power Electronics Conference (IPEC-Himeji 2022-ECCE Asia), pp. 736–740, 2022.
- [6] Y. Wu, K. Choksi, M. ul Hassan, and F. Luo, "An extendable and accurate high-frequency modelling of three-phase cable for prediction of reflected wave phenomenon," in 2022 IEEE Applied Power Electronics Conference and Exposition (APEC), pp. 944–950, 2022.
- [7] A. B. Mirza, A. I. Emon, S. S. Vala, and F. Luo, "A comprehensive analysis of current spikes in a split-phase inverter," in 2022 IEEE Applied Power Electronics Conference and Exposition (APEC), pp. 1580–1585, 2022.
- [8] P. S. Crovetti and F. Fiori, "A critical assessment of the closed-loop bulk current injection immunity test performed in compliance with iso 11452-4," *IEEE Transactions on Instrumentation and Measurement*, vol. 60, no. 4, pp. 1291–1297, 2011.
- [9] S. M. Satav and V. R. Sarma, "Mil-std-461 f-a study report," in 2008 10th International Conference on Electromagnetic Interference & Compatibility, pp. 559–563, IEEE, 2008.